

Millisecond and Binary Pulsars as Nature’s Frequency Standards.

III. Fourier Analysis and Spectral Sensitivity of Timing Observations to Low-Frequency Noise

Sergei M. Kopeikin ¹ and Vladimir A. Potapov ²

¹ *Department of Physics & Astronomy, University of Missouri-Columbia, Columbia, MO 65211, USA*

² *PRAO, ASC FIAN, Leninskii Prospect, 53, Moscow 117924, Russia*

Accepted.....200... ; Received200... ; in original form200...

ABSTRACT

Millisecond and binary pulsars are the most stable natural frequency standards which allow the introduction of modified versions of universal and ephemeris time scales based on the intrinsic rotation of pulsar and on its orbital motion around the barycentre of a binary system. The measured stability of these time scales depends on numerous physical phenomena which affect the rotational and orbital motion of the pulsar and observer on the Earth, perturb the propagation of electromagnetic pulses from the pulsar to the observer, and bring about random fluctuations in the rate of time measured by an atomic clock used as a primary time reference in timing observations. Over long time intervals the main reason for the instability of the pulsar time scales is the presence of correlated, low-frequency timing noise in residuals of times of arrivals (TOA) of electromagnetic signals from the pulsar which has both astrophysical and geophysical origins. Hence, the timing noise can carry important physical information about the interstellar medium, the interior structure of the pulsar, stochastic gravitational waves coming from the early universe and/or binary stars, etc. Each specific type of low-frequency noise can be described in a framework of the power law spectrum model. Although data processing of pulsar timing observations in the time domain seems to be the most informative, it is also important to know to which spectral bands single and binary pulsars, considered as detectors of the low-frequency noise signal, are the most sensitive. A solution to this problem may be reached only if the parallel processing of timing data in the frequency domain is fulfilled. This requires a development of the Fourier analysis technique for an adequate interpretation of data contaminated by the correlated noise with the noise spectrum which is divergent at low frequencies. The given problem is examined in the present article.

Key words: methods: data analysis - methods: statistical - pulsars: general, binary

1 INTRODUCTION

It is well known that millisecond and binary pulsars provide an excellent means for testing the theory of general relativity (Taylor & Weisberg 1982, 1989, van Straten *et al.* 2001, Weisberg & Taylor 2003, Kramer *et al.* 2003). Pulsar timing is a powerful tool for exploring the structure of the interstellar medium (Rickett 1990, 1996, Shishov 2002) and for investigating the interior of neutron stars (Cordes & Greenstein 1981, Kaspi *et al.* 1994) as well as setting an upper limit on the energy density of gravitational radiation produced in the early universe and/or by the orbital motion of binaries (Kaspi, Thorsett & Dewey 1996, McHugh *et al.* 1997, Kopeikin 1997a, Kopeikin 1999a, Kopeikin & Potapov 2000, Lommen 2002, Jaffe and Backer 2003). Physical process

of pulsar's intrinsic rotation around its axis has been proposed and used (Backer *et al.* 1982, Il'in *et al.* 1986, Rawley *et al.* 1987, Guinot & Petit 1991, Matsakis *et al.* 1997) as a new time reference (PT scale), analogous to the universal time (UT) in time-keeping metrology. The UT is based on observation of the Earth's diurnal rotation. The rate of the atomic time scale UTC is regulated by introduction of leap seconds to reproduce the rate of UT and eliminate the secular difference between the uniform atomic time scale TAI and UT (Kovalevsky and Seidelmann 2004). Quite recently, a new astronomical time reference (BPT scale) spread out over extremely long intervals (approaching 50-100 years) has been suggested (Petit & Tavella 1996) and its stability have been carefully examined by Ilyasov *et al.* (1998) and by Kopeikin (1999). BPT scale is derived from the orbital motion of a pulsar in a binary system and represents an analogue of ephemeris time (ET) in classical astronomy as based on the orbital motion of the Earth around the Sun (or the Moon around the Earth) and introduced by Newcomb (1898) at the end of the last century.

An adequate analysis of the timing data requires a deeper understanding of the nature of the noise process present in pulsar timing residuals. As soon as the autocovariance function of the noise process is known, analysis in the time domain becomes possible. Time domain analysis is the most informative since the observed stochastic process is not stationary and includes a non-stationary component which contribution to the parameters' estimates can be important (Groth 1975, Cordes 1978, 1980; Kopeikin 1997b). Because pulsar timing observations are conducted over relatively long time intervals, the white noise from errors in measuring TOA of pulsar's pulses is suppressed by the presence of a number of correlated, low-frequency ("red") noise processes having different spectra and intensities. Henceforth, we are mainly interested in analysing the red noise.

A simple, but realistic mathematical model for the red noise has been developed by Kopeikin (1997b). The model is based on the shot noise approximation with autocovariance function depending on both stationary and non-stationary components. The given model elucidates a rather remarkable fact (Kopeikin 1999b), namely, that the timing residuals as well as variances of some spin-down and all orbital parameters are not affected by the non-stationary component of the red noise at all because its contribution is filtered out by the fitting procedure based on the least square method. This observation justifies and puts on a firm ground the Fourier analysis of TOA residuals and variances of fitting parameters in the frequency domain which is normally done under implicit assumption that the non-stationary component of the autocovariance function is either absent or unimportant. We conclude that the Fourier analysis gives unbiased information about the noise process itself and permits us to reveal which frequency harmonics in the spectral expansion of the stochastic process of the pulsar timing observations are the most substantial.

Any low-frequency noise can be approximately characterized by the power-law spectrum $S(f) \sim f^{-n}$ where the spectral (integer) index $n \geq 1$. It is obvious that the spectrum has a singularity at zero frequency. Hence, the energy of TOA residuals comprised in such noise should formally have infinite value because the integral over all frequencies from zero to infinity taken from $S(f) \sim f^{-n}$ is divergent. Clearly, this has no physical meaning, and one has to resort to special mathematical methods in order to avoid this illicit divergency. There are two standard mathematical methods for curing this flaw. The first method consists in the analytical continuation of the spectrum by formally changing it from $S(f) \sim f^{-n}$ to $S(f, A) \sim f^{-(n+A)}$ where A is a purely imaginary parameter different from zero. Such a model of the analytically continued spectrum gives convergent integrals which coincide everywhere on the real axis with the integrals from the original spectrum $S(f) \sim f^{-n}$, except for the point $f = 0$. In order to prescribe a physical meaning to such integrals, we have to expand them in a Laurent series with respect to the parameter A and take the finite part of the expansion for $A = 0$. Such procedure has been used, in particular, by Kopeikin (1997a) for regularization of the autocovariance function of stochastic noise of the primordial gravitational wave background having formally divergent spectrum $S(f) \sim f^{-5}$ (Sazhin 1978, Detweiler 1979,

Mashhoon 1982, 1985, Bertotti *et al.* 1983, Mashhoon & Seitz 1991) and for setting an upper limit on the energy density of this background noise in the ultra-low frequency domain.

The procedure of analytic continuation of divergent integrals is mathematically rigorous and represents theoretically a powerful tool which gives well-defined and self-consistent mathematical results (Gel'fand & Shilov 1964). However, for researchers doing numerical computations the second method of regularization of singular spectra is preferable and more useful practically. It is based on the infrared cutoff of all divergent integrals at the frequency $f_{\text{cutoff}} = \varepsilon$, where $\varepsilon \ll 1$ is constant. The infrared cutoff technique requires corresponding modification of the power-law spectrum of the red noise in order to eliminate the dependence of the fitting parameters and the autocovariance function of the noise on the *ad hoc* introduced frequency cutoff ε . We shall prove that this modification consists of subtracting from the original power-law spectrum the infinite series of the frequency-dependent Dirac's delta function and its derivatives with numerical coefficients which are functions of the cutoff frequency ε . Such modification of the spectrum preserves the structure of the most, generally accepted, autocovariance functions and, as a consequence, does not change results of the numerical processing of signals in time domain. In addition, the infinite delta-function dependent part of the modified spectrum is rapidly convergent and accounting for contribution of few first terms is sufficient in practice. This second method of regulariazation of red spectra being divergent in the infrared frequency domain is worked out in the present paper.

In what follows, it is more convenient for mathematical purposes to express results in terms of units in which frequency and time are dimensionless. For instance, in binary pulsars, it is preferable for symbolic calculations to measure time in units of orbital frequency, $n_b = 2\pi/P_b$, where P_b is the orbital period of the binary system. In these units, frequency f is measured in terms of $1/P_b$, and dimensionless time is the pulsar's mean orbital anomaly $u = n_b t$ where t is time measured in SI units.

2 REGULARIZED SPECTRUM OF LOW-FREQUENCY NOISE

Any gaussian low-frequency noise is completely characterized by the autocovariance function which describes the correlation between two values of stochastic process separated by the arbitrary time interval $u = n_b(t_2 - t_1)$. The autocovariance function usually consists of two algebraically independent parts characterizing separately a stationary, $R^-(u)$, and a non-stationary, $R^+(u)$, component of the noise. Complete expressions of the autocovariance functions for various examples of low-frequency noise have been derived by Kopeikin (1997b), where the shot noise approximation of a stochastic process has been used. Although both stationary and non-stationary components of the autocovariance function are important for a comprehensive treatment of observations, we are dealing in the present paper only with the stationary part since the non-stationary component of the red noise is filtered out by the least square method (Kopeikin 1999b).

The stationary part of the authocovariance function can be transformed into the spectral density of noise, $S(f)$, by means of the Wiener-Khintchine theorem

$$R^-(u) = 2 \int_0^\infty S(f) \cos(2\pi fu) df, \quad (1)$$

where u is the dimensionless time and f is the dimensionless Fourier frequency. If the (constant) intensity of noise is denoted by h_n then the autocovariance function of low-frequency (correlated) noise is determined by the expression (Kopeikin 1997b)

$$\begin{cases} C_n h_n |u|^{n-1}, & n = 2, 4, 6, \dots, \text{random walk noise} \\ C_n h_n u^{n-1} \ln |u|, & n = 1, 3, 5, \dots, \text{flicker noise} \end{cases} \quad (2)$$

where C_n is a numerical constant of normalization.

Functions, which might be appropriate candidates for the spectrum of noise processes with the foregoing autocovariance functions, are $S(f) \sim h_n f^{-n}$ where n is integer. However, integrals (1) from such power-law functions are divergent because of non-physical singularity of the spectrum at zero frequency. For this reason, a regularization technique should be used because we don't usually know the asymptotic low-frequency behaviour of the spectrum and can not treat the extremely low-frequency domain adequately.

To develop the regularization method the power spectrum $S(f)$ of the noise should be defined using the truncated Fourier transform of the autocovariance function with the lower cutoff frequency $f_{\text{cutoff}} = \varepsilon$. Specifically, we require that the truncated cosine Fourier transform of $S(f)$ must give the stationary part of the original autocovariance functions (2) without any additional contributions which might come up from the cutoff-frequency lower limit of the integral and bias the estimates of the fitting parameters. Let us guess that this requirement can be satisfied with the specific model of the red-noise spectrum $S(f)$ represented by the formula

$$S(f) = \begin{cases} h_n \left[\frac{1}{(2\pi f)^n} + \sum_{k=0}^{\infty} B_{2k}(\varepsilon) \varepsilon^{2k} \delta^{(2k)}(f - \varepsilon) \right], & \text{if } f \geq \varepsilon \\ 0, & \text{otherwise} \end{cases} \quad (3)$$

where the spectral index of noise $n = 1, 2, \dots, 6$, the constant parameter h_n is the strength of noise, quantities $B_k(\varepsilon)$ are constant numerical coefficients being defined later, and $\delta^{(k)}(f - \varepsilon)$ denotes the n -th derivative with respect to f of the Dirac delta-function $\delta(f - \varepsilon)$. The Dirac delta function is defined according to the condition (Korn & Korn 1968)

$$\int_a^b f(x) \delta(x - X) dx = \begin{cases} 0, & \text{if } X < a, \text{ or } X > b, \\ \frac{1}{2} f(X + 0), & \text{if } X = a, \\ \frac{1}{2} f(X - 0), & \text{if } X = b, \\ \frac{1}{2} [f(X - 0) + f(X + 0)], & \text{if } a < X < b, \end{cases} \quad (4)$$

where $f(x)$ is an arbitrary function being such that the unilateral limits $f(X - 0)$ and $f(X + 0)$ exist. The proposed form of the low-frequency spectrum $S(f)$ will be acceptable if the coefficients $B_k(\varepsilon)$ can be uniquely determined by the condition that the cosine Fourier transform of $S(f)$ gives the stationary part of the autocovariance function of a corresponding low-frequency noise shown in Eq. (2). This statement is valid and its consistency can be proven by making use of straightforward mathematical calculations. As an example, we show how to determine the several first coefficients $B_k(\varepsilon)$ in the event of flicker noise in pulsar's rotational phase which has the spectral index $n = 1$. Coefficients $B_k(\varepsilon)$ for noises having other spectral indices will be displayed in this section without proof (which is rather easy).

The stationary part of the autocovariance function $R^-(\tau)$ of the flicker noise in the pulsar's phase is equal to $h_1 \pi^{-1} \log |u|$. According to the definition of the spectrum, accepted in the present paper, we should have

$$R^-(u) = 2 \int_{\varepsilon}^{\infty} S(f) \cos(2\pi f u) df, \quad (5)$$

where the integral has been truncated at the cutoff frequency $\varepsilon \ll 1$ to eliminate its divergency

at the point $f = 0$. Substituting $S(f)$ from Eq. (3) with $n = 1$ on right hand side of Eq. (5) and taking the integral we get

$$R^-(u) = -\frac{h_1}{\pi} \text{Ci}(2\pi\varepsilon|u|) + h_1 \cos(2\pi\varepsilon u) \sum_{k=0}^{\infty} (-1)^k B_{2k}(\varepsilon) (2\pi\varepsilon u)^{2k}, \quad (6)$$

where $\text{Ci}(x)$ is the cosine integral, and we have used the formula (Korn & Korn 1968)

$$2 \int_{\varepsilon}^{\infty} \delta^{(2k)}(f - \varepsilon) \cos(2\pi f u) df = \frac{d^{2k}}{d\varepsilon^{2k}} \cos(2\pi\varepsilon u) = (-1)^k (2\pi u)^{2k} \cos(2\pi\varepsilon u). \quad (7)$$

A Taylor expansion of the cosine integral and $\cos(2\pi\varepsilon u)$ in the right hand side of the expression (6) with respect to small parameter ε yields

$$R^-(u) = \frac{h_1}{\pi} [-\log|u| - \gamma - \log(2\pi\varepsilon)] + h_1 \left\{ B_0(\varepsilon) + (2\pi\varepsilon u)^2 \left[\frac{1}{4\pi} - \frac{1}{2} B_0(\varepsilon) - B_2(\varepsilon) \right] \right\} + O(\varepsilon^4). \quad (8)$$

Since by definition $R^-(u)$ must be equal to $-h_1 \pi^{-1} \log|u|$, we find from Eq. (8)

$$B_0(\varepsilon) = \frac{\gamma}{\pi} + \frac{\log(2\pi\varepsilon)}{\pi}, \quad B_2(\varepsilon) = \frac{1}{4\pi} - \frac{\gamma}{2\pi} - \frac{\log(2\pi\varepsilon)}{2\pi}, \quad B_4(\varepsilon) = O(\varepsilon^4). \quad (9)$$

We believe that for practical purposes it is enough to account for the coefficient $B_0(\varepsilon)$ only, since all other residual terms that appear are multiplied by the factor $2\pi\varepsilon u$, which is expected to be negligibly small under usual circumstances, because of the smallness of the product εu . From the formally mathematical point of view the smaller the cutoff frequency ε the more exact is our approximation. However, one should take into account that the real spectrum of the low-frequency noise can have the low-frequency behaviour different from the power law and our approximation will not get better for a very small value of ε . In other words the residual terms in the model of the spectrum under discussion are model dependent. Had we chosen another model for the spectrum having different behaviour as the frequency approaches zero the residual terms would look different. What model of the low frequency noise works better in the procedure of fitting parameters of the pulsar is an interesting question for further discussion. We emphasize however that the definition of the low-frequency noise spectrum in terms of the power-law model amended by the series of delta-functions and its derivatives makes the estimates of the fitting parameters not sensitive to the cutoff frequency and, thus, extrapolates the power-law model of the noise spectrum to lower frequencies than the power-law model of noise which does not account for the delta functions.

Proceeding in the same way for the set of other spectral indices we obtain the following expressions for the power spectra of low-frequency noises:

(1) Flicker noise in phase:

$$S(f) = \frac{h_1}{2\pi} \left\{ \frac{1}{f} + 2 [\gamma + \log(2\pi\varepsilon)] \delta(f - \varepsilon) \right\} + O(\varepsilon^2). \quad (10)$$

(2) Random walk in phase:

$$S(f) = \frac{h_2}{4\pi^2} \left\{ \frac{1}{f^2} - \frac{2}{\varepsilon} \delta(f - \varepsilon) \right\} + O(\varepsilon). \quad (11)$$

(3) Flicker noise in frequency:

$$S(f) = \frac{h_3}{8\pi^3} \left\{ \frac{1}{f^3} - \frac{1}{\varepsilon^2} \delta(f - \varepsilon) + [\log(2\pi\varepsilon) + \gamma - 1] \delta^{(2)}(f - \varepsilon) \right\} + O(\varepsilon^2). \quad (12)$$

(4) Random walk in frequency:

$$S(f) = \frac{h_4}{16\pi^4} \left\{ \frac{1}{f^4} - \frac{2}{3\varepsilon^3} \delta(f - \varepsilon) - \frac{2}{3\varepsilon} \delta^{(2)}(f - \varepsilon) \right\} + O(\varepsilon). \quad (13)$$

(5) Flicker noise in frequency derivative:

$$S(f) = \frac{h_5}{32\pi^5} \left\{ \frac{1}{f^5} - \frac{1}{2\varepsilon^4} \delta(f - \varepsilon) - \frac{1}{4\varepsilon^2} \delta^{(2)}(f - \varepsilon) + \frac{1}{12} \left[\gamma + \log(2\pi\varepsilon) - \frac{1}{3} \right] \delta^{(4)}(f - \varepsilon) \right\} + O(\varepsilon^2). \quad (14)$$

(6) Random walk in frequency derivative:

$$S(f) = \frac{h_6}{64\pi^6} \left\{ \frac{1}{f^6} - \frac{2}{5\varepsilon^5} \delta(f - \varepsilon) - \frac{2}{15\varepsilon^3} \delta^{(2)}(f - \varepsilon) \right\} + O(\varepsilon). \quad (15)$$

Note that the coefficient $B_4(\varepsilon) \equiv 0$ in the expression (15) for the spectrum of the random walk in the pulsar's frequency derivative.

The expressions given above indicate that there is a strong concentration of the infinite energy of the noise at the lower cutoff frequency. As we have stressed already it is a specific feature of the chosen model of the spectrum which appears because we do not know the real behaviour of the spectrum while the Fourier frequency is approaching zero. Another remark is that a formal integration of any of the foregoing spectra with spectral indices $n \geq 2$ with respect to frequency from $f = \varepsilon$ to infinity (which may be naively treated as the energy being stored in TOA residuals) gives zero value which may look surprising¹. However, it is worth noting that the whole amount of energy presents in TOA residuals can be calculated only after multiplication of the spectrum by the filter function of the fitting procedure (see section 6 below for more detail). Therefore, calculation of the total energy of residuals is more complicated and always gives a positive numerical value as expected. Similar arguments can be used in calculating variances of the fitting parameters. For example, the calculation of variances of the first several spin-down parameters in the Fourier frequency domain may give a negative numerical value for the variance (Kopeikin 1999b) which is physically meaningless. The paradox is solved if we take into account the contribution of the non-stationary part of the noise which always makes variances of the parameters numerically positive².

Pulsar timing observations can be used for the estimation of the strength and spectrum of low frequency noise present in TOA residuals. For this reason, the development of practically useful estimators of spectrum of noise are required. We are not going to consider in the present paper the question of how to construct the best possible estimators. This subject has been significantly explored by a number of other researches (see, for instance, the papers of Deeter & Boynton (1982), Deeter (1984), Taylor 1991, Matsakis *al.* 1997, Scott *et al.* 2003). Our purpose is to study the spectral dependence of TOA residuals and the variances of fitting parameters which are used in real practice.

¹ A simplest way to see this result is to notice that such integration corresponds to the value of the autocovariance function $R(u)$ taken at the point $u = 0$.

² For more detail see (Kopeikin 1999b)

In order to put our approach on a systematic basis connected to our previous works let us describe, first of all, the timing model we are dealing with.

3 TIMING MODEL

We consider a simplified, but still realistic model of arrival time measurements of pulses from a pulsar in a binary system. It is assumed that the orbit is circular, and the pulsar rotates around its own axis with angular frequency ν_p which slows down due to the electromagnetic (and other) energy losses. It also takes into account that the orbital frequency of the binary system, n_b , and its projected semimajor axis, x , have a secular drift caused by radial acceleration of the binary (Damour & Taylor 1991, Bell & Bailes 1996), its proper motion in the sky (Kopeikin 1996), and the emission of gravitational waves from the binary (Peters & Mathews 1963, Peters 1964) bringing about the gravitational radiation reaction force (Damour 1983a, Grishchuk & Kopeikin 1983). The timing model, which we work with, is described in full detail in our previous paper (Kopeikin 1999b) which particular notations we use in the present paper. Let us summarize those equations which will be useful for our analysis.

We assume that all observations of the binary pulsar are of a similar quality and weight. Then one defines the timing residuals $r(t)$ as a difference between the observed number of the pulse, \mathcal{N}^{obs} , and the number $\mathcal{N}(t, \theta)$, predicted on the ground of our best guess to the prior unknown parameters of timing model, divided by the pulsar's rotational frequency ν , that is

$$r(t, \theta) = \frac{\mathcal{N}^{obs} - \mathcal{N}(t, \theta)}{\nu}, \quad (16)$$

where $\theta = \{\theta_a, a = 1, 2, \dots, k\}$ denotes a set of k measured parameters³ which are shown in Table 1. It is worth noting that hereafter we use for the reason of convenience the time argument $u = n_b t$, that is the current orbital phase. If a numerical value of the parameter θ_a coincides with its true physical value $\hat{\theta}_a$, then the set of residuals would represent a physically meaningful noise $\epsilon(t)$, *i.e.*

$$r(t, \hat{\theta}) = \epsilon(t). \quad (17)$$

In practice, however, the true values of parameters are not attainable and we actually deal with their least square estimates θ_a^* . Therefore, the observed residuals are fitted to the expression which is a linear function of corrections to the estimates θ_a^* of a priori unknown true values of parameters $\hat{\theta}_a$. From a Taylor expansion of the timing model we work with (Kopeikin 1999b), and the fact that $r(t, \hat{\theta}) = \epsilon(t)$ one obtains

$$r(t, \theta^*) = \epsilon(t) - \sum_{a=1}^{14} \beta_a \psi_a(t, \theta^*) + O(\beta_a^2), \quad (18)$$

where the quantities $\beta_a \equiv \delta\theta_a = \theta_a^* - \hat{\theta}_a$ are the corrections to the unknown true values of parameters, and $\psi_a(t, \theta^*) = (\partial\mathcal{N}/\partial\theta_a)_{\theta=\theta^*}$ are basic fitting functions of the timing model.

In the following discussion it is convenient to regard the increments β_a as new parameters whose values are to be determined from the fitting procedure. The parameters β_a and fitting functions are summarized in Table 1 with asterisks omitted and time t is replaced in accordance to our notations and conventions by the function $u = n_b t$ which is the value of the orbital phase taken at time t . We restrict the model to 14 parameters since in practice only the first several parameters of the model

³ The number $k = 14$ in the particular timing model we are dealing with (see the paper (Kopeikin 1999b) for fuller detail.

Table 1. List of the basic functions and parameters used in the fitting procedure. Spin parameters $\delta\mathcal{N}_0, \delta\nu, \delta\dot{\nu}, \delta\ddot{\nu}, \delta\dddot{\nu}, \delta\ddddot{\nu}$, fit rotational motion of the pulsar around its own axis. Keplerian parameters $\delta x, \delta\sigma, \delta n_b$ fit the Keplerian orbital motion of the pulsar about the barycentre of the binary system. Post-Keplerian parameters $\delta\dot{x}, \delta\ddot{x}, \delta\dddot{x}, \delta\dot{n}_b, \delta\ddot{n}_b$ fit small observable deviations of the pulsar's orbit from the Keplerian motion caused by the effects of General Relativity, radial acceleration, and proper motion of the barycentre of the binary system with respect to observer.

Parameter	Fitting Function
$\beta_1 = \frac{\delta\mathcal{N}_0}{\nu}$	$\psi_1(t) = 1$
$\beta_2 = \frac{1}{n_b} \frac{\delta\nu}{\nu}$	$\psi_2(t) = u$
$\beta_3 = \frac{1}{2n_b^2} \frac{\delta\dot{\nu}}{\nu}$	$\psi_3(t) = u^2$
$\beta_4 = \frac{1}{6n_b^3} \frac{\delta\ddot{\nu}}{\nu}$	$\psi_4(t) = u^3$
$\beta_5 = \frac{1}{24n_b^4} \frac{\delta\dddot{\nu}}{\nu}$	$\psi_5(t) = u^4$
$\beta_6 = \frac{1}{120n_b^5} \frac{\delta\ddddot{\nu}}{\nu}$	$\psi_6(t) = u^5$
$\beta_7 = -\delta x \sin \sigma - \delta\sigma x \cos \sigma$	$\psi_7(t) = \cos u$
$\beta_8 = -\delta x \cos \sigma + \delta\sigma x \sin \sigma$	$\psi_8(t) = \sin u$
$\beta_9 = \frac{1}{n_b} \left(-\delta \dot{x} \cos \sigma + \delta n_b x \sin \sigma \right)$	$\psi_9(t) = u \sin u$
$\beta_{10} = \frac{1}{n_b} \left(-\delta \dot{x} \sin \sigma - \delta n_b x \cos \sigma \right)$	$\psi_{10}(t) = u \cos u,$
$\beta_{11} = \frac{1}{2n_b^2} \left(-\delta \ddot{x} \sin \sigma - \delta \dot{n}_b x \cos \sigma \right)$	$\psi_{11}(t) = u^2 \cos u$
$\beta_{12} = \frac{1}{2n_b^2} \left(-\delta \ddot{x} \cos \sigma + \delta \dot{n}_b x \sin \sigma \right)$	$\psi_{12}(t) = u^2 \sin u$
$\beta_{13} = \frac{1}{6n_b^3} \left(-\delta \dddot{x} \cos \sigma + \delta \ddot{n}_b x \sin \sigma \right)$	$\psi_{13}(t) = u^3 \sin u$
$\beta_{14} = \frac{1}{6n_b^3} \left(-\delta \dddot{x} \sin \sigma - \delta \ddot{n}_b x \cos \sigma \right)$	$\psi_{14}(t) = u^3 \cos u$

are significant in fitting the rotational and orbital phases of the pulsar over the available time span of observations.

Let us introduce auxiliary functions $\Xi_a(t)$ defined according to the formula

$$\Xi_a(t) = \sum_{b=1}^{14} L_{ab}^{-1} \psi_b(t), \quad (19)$$

where the matrix of information

$$L_{ab}(\Delta T) = \sum_{i=1}^{mN} \psi_a(t_i) \psi_b(t_i), \quad (20)$$

the matrix L_{ab}^{-1} is its inverse, and $\Delta T = NP_b$ is a total span of observational time. Functions $\Xi(t)$ are dual (Deeter 1984) to $\psi_a(t)$ because of the cross-orthonormality condition

$$\sum_{i=1}^{mN} \Xi_a(t_i) \psi_b(t_i) = \delta_{ab}. \quad (21)$$

Now suppose that we measure m equally spaced and comparably accurate arrival times for each orbit for a total of N orbital revolutions, so we have mN residuals $r_i \equiv r(t_i)$, $i = 1, \dots, mN$. Standard least squares procedure (Bard 1974) gives the best fitting solution for the estimates of the parameters β_a

$$\beta_a(\Delta T) = \sum_{i=1}^{mN} \Xi_a(t_i) \epsilon(t_i), \quad a = 1, \dots, 14. \quad (22)$$

Let the angular brackets denote an ensemble average over many stochastic realizations of the observational procedure. Hereafter, we assume that the ensemble average of the noise $\epsilon(t)$ is equal to zero. Hence, the mean value of any parameter β_a is equal to zero as well, *i.e.*

$$\langle \epsilon(t) \rangle = 0, \quad \text{and} \quad \langle \beta_a \rangle = 0. \quad (23)$$

The covariance matrix $M_{ab} \equiv \langle \beta_a \beta_b \rangle$ of the parameter estimates is given by the expression

$$M_{ab}(\Delta T) = \sum_{i=1}^{mN} \sum_{j=1}^{mN} \Xi_a(t_i) \Xi_b(t_j) R(t_i, t_j), \quad (24)$$

where $R(t_i, t_j) = \langle \epsilon(t_i) \epsilon(t_j) \rangle$ is the autocovariance function of the stochastic process $\epsilon(t)$. The covariance matrix is symmetric (that is, $M_{ab} = M_{ba}$), elements of its main diagonal give variations (dispersions) of measured parameters $\sigma_{\beta_a} \equiv M_{aa} = \langle \beta_a^2 \rangle$, and the off-diagonal terms represent the degree of statistic covariance (correlation) between them. The covariance matrix consists of two additive components M_{ab}^+ and M_{ab}^- describing contributions from the non-stationary and stationary parts of autocovariance function $R(t_i, t_j)$ respectively. Explicit expressions for the matrix M_{ab} can be found in the paper (Kopeikin 1999b) wherein we have done all our calculations in the time domain. Only M_{ab}^- admits the transformation to the frequency domain and this Fourier transform will be discussed in subsequent sections along with particular spectral properties of M_{ab}^- .

Subtraction of the adopted model from the observational data leads to the residuals which are dominated by the random fluctuations only. An expression for the mean-square residuals after subtracting the best-fitting solution for the estimates (22) is given by the formula

$$\langle r^2(\Delta T) \rangle = \frac{1}{mN} \sum_{i=1}^{mN} \sum_{j=1}^{mN} K(t_i, t_j) R(t_i, t_j), \quad (25)$$

where the function

$$K(t_i, t_j) = \delta_{ij} - \sum_{a=1}^{14} \Xi_a(t_i) \psi_a(t_j), \quad (26)$$

is called the filter function (Blandford *et al.* 1984). We have proved (Kopeikin 1999b) that the post-fit residuals depend only on the stationary part of the noise (even in the case when the non-stationary part of the autocovariance function is present) which means that Eq. (25) can be written down as

$$\langle r^2(\Delta T) \rangle = -\frac{1}{mN} \sum_{a=1}^{14} \sum_{b=1}^{14} L_{ab}^{-1} \left[\sum_{i=1}^{mN} \sum_{j=1}^{mN} \psi_a(t_i) \psi_b(t_j) R^-(t_i, t_j) \right]. \quad (27)$$

For this reason, methods of spectral analysis in frequency domain can be applied for analyzing

residuals without any restrictions. Let us note that the explicit dependence of TOA residuals on the total span of observations is contained in (Kopeikin 1999b).

4 FOURIER TRANSFORM OF FITTING FUNCTIONS

We define the Fourier transform of the fitting functions $\psi_a(t)$ as

$$\tilde{\Psi}_a(f, m, N) = \sum_{j=1}^{mN} \psi_a(t_j) \exp(-2\pi i f t_j), \quad (28)$$

where f is the Fourier frequency measured in units inversly proportional to the units of measurement of time t . We measure time in units of the orbital phase $u = n_b t$, that is in radians. Then the frequency $\omega = 2\pi f$ is dimensionless and is measured in units of the orbital frequency n_b . One notes the Fourier transform of the fitting functions depends on three arguments: the Fourier frequency f , the total number of orbital revolutions N , and the rate of observations m .

When the total number of observational points, mN , is large enough we can approximate the sum in Eq. (28) by the integral (Kopeikin 1999b)

$$\tilde{\Psi}_a(\omega, m, N) = \frac{m}{2\pi} \tilde{\psi}_a(\omega, N), \quad (29)$$

$$\tilde{\psi}_a(\omega, N) = \int_{-\pi N}^{\pi N} \psi_a(u) \exp(-i\omega u) du. \quad (30)$$

We note that $\tilde{\psi}_a(-\omega) = \tilde{\psi}_a^*(\omega)$, where the asterisk denotes a complex conjugation. Replacing the sum over observational points by the integral with respect to time (the orbital phase) makes our calculations equivalent to the case of continuous observations with uniform distribution over time.

The following formulae are also of use in practical computations

$$\tilde{\psi}_a(\omega, N) = \begin{cases} 2 \int_0^{\pi N} \psi_a(u) \cos(\omega u) du, & \text{if index } a = 1, 3, 5, \dots \\ -2i \int_0^{\pi N} \psi_a(u) \sin(\omega u) du, & \text{if index } a = 2, 4, 6, \dots \end{cases} \quad (31)$$

These expressions shows that the fitting functions with odd indices are real and those with even ones are complex.

Let us denote $T = \pi N$ and $z = \omega T$. One notices that T relates to the total span of observation using equation $T = n_b \Delta T / 2$. The Fourier transform of fitting functions takes the form

$$\tilde{\psi}_1(\omega) = 2T \tilde{\phi}_1(z), \quad (32)$$

$$\tilde{\psi}_2(\omega) = 2iT^2 \tilde{\phi}_2(z), \quad (33)$$

$$\tilde{\psi}_3(\omega) = 2T^3 \tilde{\phi}_3(z), \quad (34)$$

$$\tilde{\psi}_4(\omega) = 2iT^4 \tilde{\phi}_4(z), \quad (35)$$

$$\tilde{\psi}_5(\omega) = 2T^5 \tilde{\phi}_5(z), \quad (36)$$

$$\tilde{\psi}_6(\omega) = 2iT^6 \tilde{\phi}_6(z), \quad (37)$$

$$\tilde{\psi}_7(\omega) = T \left[\tilde{\phi}_1(z + T) + \tilde{\phi}_1(z - T) \right], \quad (38)$$

$$\tilde{\psi}_8(\omega) = iT \left[\tilde{\phi}_1(z + T) - \tilde{\phi}_1(z - T) \right], \quad (39)$$

$$\tilde{\psi}_9(\omega) = T^2 \left[\tilde{\phi}_2(z - T) - \tilde{\phi}_2(z + T) \right], \quad (40)$$

$$\tilde{\psi}_{10}(\omega) = iT^2 \left[\tilde{\phi}_2(z - T) + \tilde{\phi}_2(z + T) \right], \quad (41)$$

$$\tilde{\psi}_{11}(\omega) = T^3 \left[\tilde{\phi}_3(z + T) + \tilde{\phi}_3(z - T) \right], \quad (42)$$

$$\tilde{\psi}_{12}(\omega) = iT^3 \left[\tilde{\phi}_3(z + T) - \tilde{\phi}_3(z - T) \right], \quad (43)$$

$$\tilde{\psi}_{13}(\omega) = T^4 \left[\tilde{\phi}_4(z - T) - \tilde{\phi}_4(z + T) \right], \quad (44)$$

$$\tilde{\psi}_{14}(\omega) = iT^4 \left[\tilde{\phi}_4(z - T) + \tilde{\phi}_4(z + T) \right]. \quad (45)$$

where functions $\phi_a(z)$ ($a = 1, 2, \dots, 6$) have the following form

$$\tilde{\phi}_1(z) = \frac{\sin z}{z}, \quad (46)$$

$$\tilde{\phi}_2(z) = \frac{\cos z}{z} - \frac{\sin z}{z^2}, \quad (47)$$

$$\tilde{\phi}_3(z) = \frac{\sin z}{z} + \frac{2 \cos z}{z^2} - \frac{2 \sin z}{z^3}, \quad (48)$$

$$\tilde{\phi}_4(z) = \frac{\cos z}{z} - \frac{3 \sin z}{z^2} - \frac{6 \cos z}{z^3} + \frac{6 \sin z}{z^4}, \quad (49)$$

$$\tilde{\phi}_5(z) = \frac{\sin z}{z} + \frac{4 \cos z}{z^2} - \frac{12 \sin z}{z^3} - \frac{24 \cos z}{z^4} + \frac{24 \sin z}{z^5}, \quad (50)$$

$$\tilde{\phi}_6(z) = \frac{\cos z}{z} - \frac{5 \sin z}{z^2} - \frac{20 \cos z}{z^3} + \frac{60 \sin z}{z^4} + \frac{120 \cos z}{z^5} - \frac{120 \sin z}{z^6}. \quad (51)$$

Simple inspection reveals that these functions are linear combinations of the spherical Bessel functions $j_a(z)$ defined as (Korn & Korn 1968, section 21.8-8)

$$j_a(z) = z^a \left(-\frac{1}{z} \frac{d}{dz} \right)^a \frac{\sin z}{z}, \quad (a = 0, 1, 2, \dots). \quad (52)$$

The Bessel functions have a polynomial behaviour⁴ near the point $z = 0$, and then oscillate with monotonically decreasing amplitude. Asymptotic expansion of the spherical Bessel functions for large values of the variable z (that is directly proportional to the Fourier frequency) are given by the formula

⁴ The function $j_a(z) = \frac{z^a}{(2a+1)!!} + O(z^{a+2})$ for $z \ll 1$ ($a = 0, 1, 2, \dots$).

$$j_a(z) \approx \frac{\sin\left(z - \frac{\pi a}{2}\right)}{z}. \quad (53)$$

It is worth emphasizing that the maximum value for any of these functions can not be larger than 1.

The fitting functions $\tilde{\phi}_a(z)$, expressed in terms of the spherical Bessel functions, assume the form

$$\tilde{\phi}_1(z) = j_0(z), \quad (54)$$

$$\tilde{\phi}_2(z) = -j_1(z), \quad (55)$$

$$\tilde{\phi}_3(z) = \frac{1}{3}j_0(z) - \frac{2}{3}j_2(z), \quad (56)$$

$$\tilde{\phi}_4(z) = -\frac{3}{5}j_1(z) + \frac{2}{5}j_3(z), \quad (57)$$

$$\tilde{\phi}_5(z) = \frac{1}{5}j_0(z) - \frac{4}{7}j_2(z) + \frac{8}{35}j_4(z), \quad (58)$$

$$\tilde{\phi}_6(z) = -\frac{3}{7}j_1(z) + \frac{4}{9}j_3(z) - \frac{8}{63}j_5(z). \quad (59)$$

5 FOURIER TRANSFORM OF THE COVARIANCE MATRIX

In order to calculate the covariance matrix we need to know the Fourier transform of the dual functions $\Xi_a(t)$. The transform is defined in accordance with definition (19) of the dual functions and takes the form

$$\tilde{\Xi}_a(f, m, N) = \sum_{c=1}^{14} L_{ac}^{-1} \tilde{\Psi}_c(f, m, N), \quad (60)$$

and the cross-orthonormal condition in the frequency domain is given by the integral

$$\int_0^\infty \tilde{\Xi}_a(f, m, N) \tilde{\Psi}_b(f, m, N) df = \frac{1}{2} \delta_{ab}. \quad (61)$$

In the limit of continuous observations it is convenient to introduce the matrix $C_{ab} = \frac{2\pi}{m} L_{ab}$ instead of the information matrix L_{ab} . The explicit expression for the matrix C_{ab} is given by the integral:

$$C_{ab} = \int_{-\pi N}^{\pi N} \psi_a(u) \psi_b(u) du, \quad (62)$$

and the result of evaluation of this integral is given in the paper by Kopeikin (1999b) in Tables 5 and 6. Then we have $L_{ab}^{-1} = (2\pi/m) C_{ab}^{-1}$, and the Fourier transform of the dual function $\tilde{\Xi}(f)$ can be recast as

$$\tilde{\Xi}_a(f, N) = \sum_{b=1}^{14} C_{ab}^{-1} \tilde{\psi}_b(f, N). \quad (63)$$

Hence, comparing the eq. (63) with (60) one concludes that in the limit of continuous observations the Fourier transform of the dual functions depends only on the Fourier frequency and the total number of orbital revolutions as was expected. It is more insightful to express the dual functions (63) in terms of the spherical Bessel functions (52). The expressions obtained are rather unwieldy, and, for this reason they are given in Appendix A.

Making use of the definition of the Fourier transforms of the stationary part of the autocovariance function (5) and the dual functions (60) we obtain the stationary part of the covariance matrix $M_{ab}^-(m, N)$ (see Eq. (24) for its definition) expressed as follows

$$M_{ab}^- = \int_{\varepsilon}^{\infty} S(f) H_{ab}(f, m, N) df, \quad (64)$$

where $H_{ab}(f, m, N)$ is the transfer function given by the expression

$$H_{ab}(f, m, N) = \tilde{\Xi}_a(f, m, N) \tilde{\Xi}_b^*(f, m, N) + \tilde{\Xi}_a^*(f, m, N) \tilde{\Xi}_b(f, m, N), \quad (65)$$

and an asterisk denotes complex conjugation. For numerical computations of M_{ab}^- the following formula can be used in practical computations

$$M_{ab}^-(m, N) = \frac{h_n}{(2\pi)^n} \int_{\varepsilon}^{\Lambda} H_{ab}(f, m, N) f^{-n} df + \quad (66)$$

$$\frac{1}{2} h_n \left[B_0(\varepsilon) H_{ab}(\varepsilon, m, N) + \varepsilon^2 B_2(\varepsilon) H_{ab}^{(2)}(\varepsilon, m, N) + \varepsilon^4 B_4(\varepsilon) H_{ab}^{(4)}(\varepsilon, m, N) + \dots \right],$$

where derivatives of H_{ab} are taken with respect to the Fourier frequency, ellipses denote terms of negligible influence on the result of the computation, and Λ is the upper cutoff frequency arising from the sampling theorem and is inversely proportional to the minimal time between subsequent observational sessions. We emphasize that the matrix $M_{ab}^-(m, N)$ does not depend on the lower cutoff frequency because all contributions from the lower limit of the integral in Eq. (66) are canceled out by corresponding terms from the series.

6 FOURIER TRANSFORM OF THE FILTER FUNCTION

Timing residuals are expressed in terms of the Fourier transform of the filter function. Employing eqs. (5), (27), and (30) yields for the residuals

$$\langle r^2 \rangle = 2 \int_{\varepsilon}^{\infty} S(f) K(f, m, N) df, \quad (67)$$

where is the Fourier transform of the filter function (26)

$$K(f, m, N) = 1 - \frac{1}{2mN} \sum_a^{14} \left[\tilde{\Xi}_a(f, m, N) \tilde{\Psi}_a^*(f, m, N) + \tilde{\Xi}_a^*(f, m, N) \tilde{\Psi}_a(f, m, N) \right], \quad (68)$$

is the Fourier transform of the filter function defined in Eq. (26). In the limit of continuous observations there is no dependence on the frequency of observations, m , so that one obtains

$$K(f, N) = 1 - \frac{1}{4T} \sum_a^{14} \left[\tilde{\Xi}_a(f, N) \tilde{\psi}_a^*(f, N) + \tilde{\Xi}_a^*(f, N) \tilde{\psi}_a(f, N) \right]. \quad (69)$$

Plots of the Fourier transform (69) of the filter function $K(f)$ are shown in Appendix D for different numbers of orbital revolutions N . In any case the filter function is approximately equal to 1 until the frequency is higher than $1/(\Delta T)$, and rapidly decreases in amplitude as the frequency approaches zero. We also note that the plot of the Fourier transform of the filter function clearly

shows the additional dip near the orbital frequency. The dips near zero and orbital frequencies get narrower as the number of observational points increases.

7 SPECTRAL SENSITIVITY OF TIMING OBSERVATIONS OF MILLISECOND AND BINARY PULSARS

Analytical expressions and graphical representations of Fourier transforms of dual functions and timing residuals help us to understand in more detail the spectral sensitivity of single and binary pulsars to different frequency bands in the spectral decomposition of the noise. First, let us consider behaviour of the Fourier transform of fitting functions near zero and the orbital frequencies.

It is easy to confirm after making use of Taylor expansion of exponential function in (30) near $\omega \simeq 0$ that

$$\tilde{\psi}_a(\omega) = \begin{cases} C_{a1} - \frac{1}{2}\omega^2 C_{a3} + \frac{1}{24}\omega^4 C_{a5} + \omega^6 p_a, & \text{if } a=1,3,5,\dots \\ i \left(-\omega C_{a2} + \frac{1}{6}\omega^3 C_{a4} - \frac{1}{120}\omega^5 C_{a6} + \omega^7 p_a \right), & \text{if } a=2,4,6,\dots, \end{cases} \quad (70)$$

where p_a is a residual term depending only on the total number of orbital revolutions, N . A Taylor expansion of the Fourier transform of the fitting functions near the orbital frequency yields

$$\tilde{\psi}_a(\omega) = \begin{cases} C_{a7} + (\omega - 1)C_{a9} - \frac{(\omega-1)^2}{2}C_{a,11} - \frac{(\omega-1)^3}{6}C_{a,13} + (\omega - 1)^4 q_a, & \text{if } a=1,3,\dots \\ i \left[-C_{a8} + (\omega - 1)C_{a,10} + \frac{(\omega-1)^2}{2}C_{a,12} - \frac{(\omega-1)^3}{6}C_{a,14} + (\omega - 1)^4 q_a \right], & \text{if } a=2,4,\dots, \end{cases} \quad (71)$$

where q_a is a residual term depending only on the total number of orbital revolutions, N (recall that the frequency is measured in units of the orbital frequency n_b). Applying to Eqs. (70)–(71) the definition of the dual functions (63) in the limit of continuous observations yields the asymptotic behaviour of the dual functions

$$\tilde{\Xi}_a(\omega) = \begin{cases} \delta_{a1} - \frac{1}{2}\omega^2 \delta_{a3} + \frac{1}{24}\omega^4 \delta_{a5} + \omega^6 P_a, & \text{if } a=1,3,5,\dots \\ i \left(-\omega \delta_{a2} + \frac{1}{6}\omega^3 \delta_{a4} - \frac{1}{120}\omega^5 \delta_{a6} + \omega^7 P_a \right), & \text{if } a=2,4,6,\dots, \end{cases} \quad (72)$$

near zero frequency, and

$$\tilde{\Xi}_a(\omega) = \begin{cases} \delta_{a7} + (\omega - 1)\delta_{a9} - \frac{(\omega-1)^2}{2}C_{a,11} - \frac{(\omega-1)^3}{6}\delta_{a,13} + (\omega - 1)^4 Q_a, & \text{if } a=1,3,\dots \\ i \left[-\delta_{a8} + (\omega - 1)\delta_{a,10} + \frac{(\omega-1)^2}{2}\delta_{a,12} - \frac{(\omega-1)^3}{6}\delta_{a,14} + (\omega - 1)^4 Q_a \right], & \text{if } a=2,4,\dots, \end{cases} \quad (73)$$

near the orbital frequency, where P_a and Q_a are residual terms. Table 2 shows the asymptotic behaviour of the residual terms of the dual functions.

Now we can study the asymptotic behaviour of the filter function $K(f)$ as defined by eq. (69). Taking into account the fact that $\sum_{b=1}^{14} C_{ab}^{-1} C_{bc} = \delta_{ac}$ where δ_{ac} is the unit matrix, we obtain

$$K(f) = \begin{cases} b_0 \cdot \omega^6, & \text{when } \omega \rightarrow 0 \\ b_1 \cdot (\omega - 1)^4, & \text{when } \omega \rightarrow 1 \end{cases} \quad (74)$$

where b_0 and b_1 are numerical constants which can be calculated precisely but are not important

for the discussion present in this section. Such a dependence of the filter function $K(f)$ on the frequency f significantly reduces the amount of the detected red-noise power below the cutoff frequency $f_{\text{cutoff}} \simeq \alpha_c T^{-1}$ and in the frequency band $1 - \alpha_b T^{-1} \leq f \leq 1 + \alpha_b T^{-1}$ lying near the orbital frequency. Here constant coefficients α_c and α_b can be determined by comparing the calculations of the mean value of the timing residuals in time and frequency domains (Kopeikin 1997a). The low Fourier frequencies in the noise power spectrum are fitted away by the polynomial fit for the spin-down parameters of the observed pulsar. The Fourier frequencies close to the orbital frequency are fitted away by the fit for the orbital parameters of the pulsar. The amount of noise power remaining in timing residuals after completion of fitting procedure ⁵ is estimated by the expressions

$$\langle r^2 \rangle = 2 \int_{\frac{\alpha_c}{T}}^{1 - \frac{\alpha_b}{T}} S(f) df + 2 \int_{1 + \frac{\alpha_b}{T}}^{\infty} S(f) df = \frac{2h_n}{(2\pi)^n} \left(\frac{\alpha_c^{1-n} T^{n-1}}{n-1} - \frac{2\alpha_b}{T} \right) + O\left(\frac{1}{T^3}\right), \quad (n > 1) \quad (75)$$

and

$$\langle r^2 \rangle = 2 \int_{\frac{\alpha_c}{T}}^{1 - \frac{\alpha_b}{T}} S(f) df + 2 \int_{1 + \frac{\alpha_b}{T}}^{\infty} S(f) df = \frac{h_1}{\pi} \left(\ln T - \frac{2\alpha_b}{T} \right) + O\left(\frac{1}{T^3}\right), \quad (n = 1) \quad (76)$$

where for the calculation of the first and the second integrals we have taken the very first terms of the spectra ⁶ given in Eqs. (10)–(15) and assumed that $\alpha_b/T \ll 1$ and $\alpha_c/T \ll 1$ so that these quantities are used as small parameters of the Taylor expansion of the integrals under calculation. We draw attention of the reader that in real signal processing the infinite-frequency limit in Eqs.(75), (76) is, in fact, inversely proportional to the sampling time of observations.

The second term in the right hand side of Eqs. (75), (76) shows amount of noise absorbed by fitting orbital parameters. It is negligibly small compared to the first term in the right hand side and can be neglected in practice. Hence, we conclude that the post-fit timing residuals can be used for the estimation of the amount of red noise and its spectrum in frequency band just from $\alpha_c T^{-1}$ up to infinity, irrespectively of whether the pulsar is binary or not. This reasoning puts on firm ground the estimates of spectral sensitivity of timing observations and the cosmological parameter Ω_g , characterizing energy density of stochastic gravitational waves in early universe, made by Kaspi *et al.* (1994) and Camilo *et al.* (1994) using observations of binary pulsars PSR B1855+09 and PSR J1713+0747 respectively.

Analysis of the spectral sensitivity of the estimates of variances of spin-down and orbital parameters is more cumbersome. We are interested in which frequencies give the biggest contribution to the variances. This is important to know, for example, if we want to use variances of certain orbital parameters for setting the fundamental upper limit on Ω_g in the ultra-low frequency domain (Kopeikin 1997a). Analytical calculations reveal the leading terms in the asymptotic expansions of the dual functions near zero frequencies which are present in Table 2. The squares of the dual functions $\tilde{\xi}_a$ appearing in eqs. (B1)–(B14) and eqs. (C1)–(C14) are rather complicated. Their behaviour is periodic with bumps both near zero and the orbital frequencies and with oscillating behaviour which amplitude is rapidly decaying far outside of these frequencies. We determined that the amount of noise absorbed by fitting of the spin-down parameters near zero frequency is essentially bigger than that near the orbital one. On the other hand, the amount of noise absorbed by fitting of the orbital parameters is substantial for the Fourier frequencies lying near the orbital frequency. Thus, there are two spectral windows in which parameter' variances of the timing model are most sensitive to the stochastic red noise and they are located near zero and the orbital frequency. These windows

⁵ It is useful to compare calculations of the residuals given in the present paper with those given in (Kopeikin 1999b).

⁶ Delta-functions and their derivatives do not contribute to the integrals in the approximation under consideration.

Table 2. Asymptotic behaviour of residual terms of the dual functions $\tilde{\Xi}_a$ near zero and orbital frequencies. Constant $h = \cos T = (-1)^N$.

Dual function	Residual term P_a	Residual term Q_a
$\tilde{\Xi}_1$	$-\frac{1}{33264}T^6$	$\frac{19}{56}T^2h$
$\tilde{\Xi}_2$	$\frac{1}{61776}T^6$	$-\frac{1}{8}T^2h$
$\tilde{\Xi}_3$	$\frac{1}{1584}T^4$	$-\frac{17}{4}h$
$\tilde{\Xi}_4$	$-\frac{1}{6864}T^4$	$-\frac{3}{4}h$
$\tilde{\Xi}_5$	$-\frac{1}{528}T^2$	$-\frac{45}{8}\frac{h}{T^2}$
$\tilde{\Xi}_6$	$\frac{1}{3120}T^2$	$\frac{33}{40}\frac{h}{T^2}$
$\tilde{\Xi}_7$	$-\frac{1}{165}T^4h$	$-\frac{1}{280}T^4$
$\tilde{\Xi}_8$	$\frac{1}{45045}T^6h$	$\frac{1}{280}T^4$
$\tilde{\Xi}_9$	$-\frac{1}{693}T^4h$	$-\frac{1}{28}T^2$
$\tilde{\Xi}_{10}$	$-\frac{1}{273}T^4h$	$\frac{1}{28}T^2$
$\tilde{\Xi}_{11}$	$-\frac{19}{693}T^2h$	$\frac{1}{28}T^2$
$\tilde{\Xi}_{12}$	$\frac{1}{9009}T^4h$	$-\frac{1}{28}T^2$
$\tilde{\Xi}_{13}$	$\frac{1}{297}T^2h$	$\frac{1}{12}$
$\tilde{\Xi}_{14}$	$\frac{31}{3861}T^2h$	$-\frac{1}{12}$

are restricted by two frequency intervals, $(0, \frac{\alpha}{T})$, and, $(1 - \frac{\alpha_-}{T}, 1 + \frac{\alpha_+}{T})$, respectively, where constant coefficients α , α_- , α_+ can be calculated by comparing calculations of variances of the fitting parameters in time and frequency domains. The variances of the fitting parameters depend only on the total span, ΔT , of observations (Kopeikin 1997b). Comparing the dependence of the variances on ΔT calculated in time domain with that calculated in the frequency domain with the integrals truncated by the two frequency windows, reveals the relative importance in contribution of different frequencies to the integrated values of the variances of the parameters given by two integrals

$$I_1 \sim h_n \int_{\varepsilon}^{\frac{\alpha}{T}} |\tilde{\Xi}_a(f)|^2 \left[\frac{1}{(2\pi f)^n} + \sum_{k=0}^{\infty} B_{2k}(\varepsilon) \varepsilon^{2k} \delta^{(2k)}(f - \varepsilon) \right] df, \tag{77}$$

and

$$I_2 \sim \frac{h_n}{(2\pi)^n} \int_{1 - \frac{\alpha_-}{T}}^{1 + \frac{\alpha_+}{T}} |\tilde{\Xi}_a(f)|^2 f^{-n} df, \tag{78}$$

The first integral describes the contribution of low frequencies to the parameter's variances. The second integral gives the contribution to the parameter's variances from the frequencies lying near the orbital frequency. It is worth emphasizing that the terms with delta functions and their derivatives in Eq. (77) cancel out all terms depending on the cutoff frequency ε and diverging as

Table 3. Comparative contribution of different frequency bands to variances of spin-down ($a = 1, 2, \dots, 6$) and orbital ($a = 7, 8, \dots, 14$) parameters β_a . Number $n = 1, 2, \dots, 6$ denotes the spectral index of corresponding red noise. Time dependence of all variances completely coincides with that which was obtained by calculations in time domain as given in (Kopeikin 1999b).

Variance of parameter	Contribution of integral I ₁	Contribution of integral I ₂
$\sigma_{\beta_1}^2$	$\sim T^{n-1}$	$\sim T^{-3}$
$\sigma_{\beta_2}^2$	$\sim T^{n-3}$	$\sim T^{-5}$
$\sigma_{\beta_3}^2$	$\sim T^{n-5}$	$\sim T^{-7}$
$\sigma_{\beta_4}^2$	$\sim T^{n-7}$	$\sim T^{-9}$
$\sigma_{\beta_5}^2$	$\sim T^{n-9}$	$\sim T^{-11}$
$\sigma_{\beta_6}^2$	$\sim T^{n-11}$	$\sim T^{-13}$
$\sigma_{\beta_7}^2$	$\sim T^{n-5}$	$\sim T^{-1}$
$\sigma_{\beta_8}^2$	$\sim T^{n-3}$	$\sim T^{-1}$
$\sigma_{\beta_9}^2$	$\sim T^{n-5}$	$\sim T^{-3}$
$\sigma_{\beta_{10}}^2$	$\sim T^{n-7}$	$\sim T^{-3}$
$\sigma_{\beta_{11}}^2$	$\sim T^{n-9}$	$\sim T^{-5}$
$\sigma_{\beta_{12}}^2$	$\sim T^{n-7}$	$\sim T^{-5}$
$\sigma_{\beta_{13}}^2$	$\sim T^{n-9}$	$\sim T^{-7}$
$\sigma_{\beta_{14}}^2$	$\sim T^{n-11}$	$\sim T^{-7}$

ε goes to zero. This cancellation has been expected since we modified the spectrum of red noise to avoid the appearance of all divergent terms which have no physical meaning. We don't give here the results of the calculation of numerical values of constants α , α_- , α_+ because they are not so important for general conclusions. The asymptotic behaviour of the dual functions near zero and the orbital frequency is enough informative to see which frequency band is the most important for giving contributions to the corresponding integrals and the parameter's variances. The time dependence of two integrals is shown in Table 3 up to a not so important constant. The behavior of the variances of the first three spin-down parameters is not physically interesting because they are contaminated and strongly biased by the presence of the non-stationary part of the red noise (Kopeikin 1997b). For the rest of the spin-down parameters one observes that the contribution of the noise energy from low frequencies to the variances of the parameters is dominating. However, the situation is not so simple in the case of the orbital parameters. One can see that in the case of red noise having spectral index $n \leq 4$, the contribution of the noise energy from the orbital frequency interval $(1 - \frac{\alpha_-}{T}, 1 + \frac{\alpha_+}{T})$ can be equal to or even bigger than that from the low frequency band. Only when the spectral index of noise is $n \geq 5$ does the contribution of the noise energy of low frequencies to the variances of orbital parameters begins to dominate.

It is worth noting that the timing noise with the spectral index $n = 5$ is produced by the cosmological gravitational wave background. The fact that for this noise low-frequencies give the

main contribution to the variances of orbital parameters confirms our early statement (Kopeikin 1997a) that the measurement of the variances of orbital parameters showing secular evolution probes the ultra-low frequency band of the cosmological gravitational wave background. Hence, these variances can be used for setting an upper limit on the cosmological parameter Ω_g in this frequency range, in contrast to timing residuals which test only the low-frequency band of the background noise as explained in (Kopeikin 1997a).

8 ACKNOWLEDGMENTS

We are grateful to N. Wex for numerous fruitful discussions which have helped to improve the presentation of this manuscript. We thank H. Lambert and A. Corman for careful reading of the manuscript and valuable comments. We are indebted to the anonymous referee for pointing out new references and for suggestions which helped to shorten and clarify the article.

REFERENCES

- Backer D.C., Kulkarni S.R., Heiles C., Davis M.M. & Goss W.M., 1982, *Nature*, **300**, 615
 Bard Y., 1974, *Nonlinear Parameter Estimation* (Academic Press: New York)
 Bell J.F. & Bailes M., 1996, *ApJ*, **456**, L33
 Bertotti B., Carr B.J. & Rees M.J., 1983, *MNRAS*, **203**, 945
 Blandford R., Narayan R. & Romani R., 1984, *J. Astrophys. Astron.*, **5**, 369
 Camilo F., Foster R.S. & Wolszczan A., 1994, *ApJ*, **437**, L39
 Cordes J.M., 1978, *ApJ*, **222**, 1006
 Cordes J.M., 1980, *ApJ*, **237**, 216
 Cordes J.M. & Greenstein, G., 1981, *ApJ*, **245**, 1060
 Damour T., 1983a, *Phys. Rev. Lett.*, **51**, 1019
 Damour T. & Taylor J.H., 1991, *ApJ*, **366**, 501
 Damour T. & Taylor J.H., 1992, *Phys. Rev. D.*, **45**, 1840
 Deeter J.E. & Boynton P.E., 1982, *ApJ*, **261**, 337
 Deeter J.E., 1984, *ApJ*, **281**, 482
 Deeter J. E., Boynton P.E., Lamb F. K. & Zylstra G., 1989, *ApJ*, **336**, 376
 Detweiler S., 1979, *ApJ*, **234**, 1100
 Doroshenko O.V. & Kopeikin S.M., 1990, *Sov. Astron.*, **34**, 496
 Doroshenko O.V. & Kopeikin S. M., 1995, *MNRAS*, **274**, 1029
 Gel'fand I.M. & Shilov G.E., 1964, *Generalized Functions: Properties and Operations* (Academic Press, New York)
 Grishchuk L.P. & Kopeikin S.M., 1983, *Sov. Astron. Lett.*, **9**, 230
 Groth E.J., 1975, *ApJ Suppl.*, **29**, 453
 Guinot B. & Petit G., 1991, *Astron. Astrophys.*, **248**, 292
 Il'in V. G., Isaev L. K., Pushkin S. B., Palii G. N., Ilyasov Y. P., Kuzmin A. D., Shabanova T. V. & Shitov Y. P., 1986, *Metrologia*, **22**, 65
 Ilyasov Yu.P., Kopeikin S.M. & Rodin A.E., 1998, *Astronomy Letters*, **24**, 228
 Jaffe A.H. & Backer D.C. 2003, *ApJ.*, **583** 616
 Kaspi V.M., Taylor J.H. & Ryba M.F., 1994, *ApJ*, **428**, 713
 Kopeikin S.M., 1988, *Cel. Mech.*, **44**, 87
 Kopeikin S.M., 1994, *ApJ*, **434**, L67
 Kopeikin S.M., 1996, *ApJ*, **467**, L93
 Kopeikin S.M., 1997a, *Phys. Rev. D*, **56**, 4455
 Kopeikin S.M., 1997b, *MNRAS*, **288**, 129
 Kopeikin S. M., 1999a, in: Proc. XXXIVth Rencontres de Moriond on "Gravitational Waves and Experimental Gravity" [Les Arcs, France, 1999] eds. by J.Trn Thanh Vn *et al.* (World Publishers, Hanoi 2000) pp. 325-330 (e-print: gr-qc/9903070)
 Kopeikin S.M., 1999b, *MNRAS*, **305**, 563
 Kopeikin S. M. & Potapov V. A. 2000, ASP Conf. Ser. 202: IAU Colloq. 177: Pulsar Astronomy - 2000 and Beyond, 117
 Korn G. A. & Korn T. A., 1968, *Mathematical Handbook for scientists and engineers* (McGraw-Hill Book Comp., New York 1968)
 Kovalevsky J. & Seidelmann P.K., 2004, *Fundamentals of Astrometry* (Cambridge Univ. Press, Cambridge 2004)
 Kramer M., Löhmer O. & Karastergiou A., 2003, in: ASP Conf. Ser. 302, Radio Pulsars, eds. M. Bailes, D. J. Nice, & S. E. Thorsett (San Francisco: ASP), 93, pp. 99-102
 Lommen A. N., 2002, in: Proc. of the 270 WE-Heraeus Seminar on Neutron Stars, Pulsars and Supernova Remnants, eds. W. Becker, H., Lesch & J. Truemper, MPE-Report 278 (e-print: astro-ph/0208572)
 Mashhoon B., 1982, *MNRAS*, **199**, 659
 Mashhoon B., 1985, *MNRAS*, **217**, 265
 Mashhoon B. & Seitz M., 1991, *MNRAS*, **249**, 84
 Matsakis D. N., Taylor J. H. & Eubanks T. M., 1997 *A&A*, **326**, 924

- McHugh M.P., Zalamansky G., Vernetto F. & Lantz E., 1996, Phys. Rev. D, **54**, 5993
 Newcomb S., 1898, Astron. Papers Am. Ephemeris Nautical Almanac, **6**, 7
 Peters P. C. & Mathews J., 1963, Phys. Rev., **131**, 435
 Peters P. C., 1964, Phys. Rev., **136**, 1224
 Petit G. & Tavella P. 1996, Astron. Astrophys., **308**, 290
 Rawley L.A., Taylor J.H., Davis M.M. & Allan D.W., 1987, Science, **238**, 761
 Rickett B. J., 1990, Ann. Rev. Astron. Astrophys., **28**, 561
 Rickett B. J., 1996, Interstellar Scattering: Observations and Interpretations, In: Pulsars, Problems and Progress, eds. S. Johnston, M.A. Walker, M. Bailes, ASP Conf. Ser. **105**, 439
 Sazhin M.V., 1978, Soviet Astronomy, **22**, 36
 Scott D. M., Finger M. H. & Wilson C. A., 2003, MNRAS, 344, 412
 Shishov V. I., 2002, Astronomical and Astrophysical Transactions, **21**, 49
 Taylor J.H., 1991, Proc. IEEE, **79**, 1054
 Taylor J.H. & Weisberg J.M., 1982, ApJ, **253**, 908
 Taylor J.H. & Weisberg J.M., 1989, ApJ, **345**, 434
 Thorsett S.E. & Dewey R.J., 1996, Phys. Rev. D, **53**, 3468
 van Straten W., Bailes M., Britton M., Kulkarni S. R., Anderson S. B., Manchester R. N. & Sarkissian, J. 2001, Nature, **412**, 158
 Weisberg J. & Taylor J. H. 2003, in: ASP Conf. Ser. 302, Radio Pulsars, eds. M. Bailes, D. J. Nice, & S. E. Thorsett (San Francisco: ASP), 93, pp. 93–98

APPENDIX A: EXPLICIT EXPRESSIONS FOR THE DUAL FUNCTIONS

In this appendix we give explicit expressions for the dual functions. Using definition (63) and elements of inverse matrix C_{ab}^{-1} from the paper (Kopeikin 1999b, Tables 5 and 6) one obtains

$$\begin{aligned} \tilde{\Xi}_1(z) = & j_0(z) + \frac{5}{2}j_2(z) + \frac{27}{8}j_4(z) + \\ & + \frac{15h}{8T} \left\{ 3 [j_1(z+T) - j_1(z-T)] - 7 [j_3(z+T) - j_3(z-T)] \right\} \\ & - \frac{45h}{8T^2} \left\{ 3 [j_0(z+T) + j_0(z-T)] - 20 [j_2(z+T) + j_2(z-T)] \right\}, \end{aligned} \quad (\text{A1})$$

$$\begin{aligned} \frac{1}{i} \tilde{\Xi}_2(z) = & -\frac{3}{T} \left[j_1(z) + \frac{7}{2}j_3(z) + \frac{55}{8}j_5(z) \right] + \\ & \frac{105h}{8T^2} \left\{ j_0(z+T) - j_0(z-T) - 5 [j_2(z+T) - j_2(z-T)] \right\} + \\ & \frac{105h}{8T^3} \left\{ 51 [j_1(z+T) + j_1(z-T)] - 154 [j_3(z+T) + j_3(z-T)] \right\}, \end{aligned} \quad (\text{A2})$$

$$\begin{aligned} \tilde{\Xi}_3(z) = & -\frac{15}{2T^2} \left[j_2(z) + \frac{9}{2}j_4(z) \right] \\ & - \frac{105h}{4T^3} \left\{ 3 [j_1(z+T) - j_1(z-T)] - 7 [j_3(z+T) - j_3(z-T)] \right\} + \\ & \frac{105h}{4T^4} \left\{ 7 [j_0(z+T) + j_0(z-T)] - 50 [j_2(z+T) + j_2(z-T)] \right\}, \end{aligned} \quad (\text{A3})$$

$$\frac{1}{i} \tilde{\Xi}_4(z) = \frac{35}{2T^3} \left[j_3(z) + \frac{11}{2}j_5(z) \right] \quad (\text{A4})$$

$$\begin{aligned}
 & -\frac{315h}{4T^4} \left\{ j_0(z+T) - j_0(z-T) - 5 [j_2(z+T) - j_2(z-T)] \right\} \\
 & -\frac{1575h}{4T^5} \left\{ 9 [j_1(z+T) + j_1(z-T)] - 28 [j_3(z+T) + j_3(z-T)] \right\},
 \end{aligned}$$

$$\tilde{\Xi}_5(z) = \frac{315}{8T^4} j_4(z) \tag{A5}$$

$$\begin{aligned}
 & +\frac{315h}{8T^5} \left\{ 3 [j_1(z+T) - j_1(z-T)] - 7 [j_3(z+T) - j_3(z-T)] \right\} \\
 & -\frac{1575h}{8T^6} \left\{ [j_0(z+T) + j_0(z-T)] - 8 [j_2(z+T) + j_2(z-T)] \right\},
 \end{aligned}$$

$$\frac{1}{i} \tilde{\Xi}_6(z) = -\frac{693}{8T^5} j_5(z) + \tag{A6}$$

$$\begin{aligned}
 & \frac{693h}{8T^6} \left\{ j_0(z+T) - j_0(z-T) - 5 [j_2(z+T) - j_2(z-T)] \right\} + \\
 & \frac{2079h}{8T^7} \left\{ 13 [j_1(z+T) + j_1(z-T)] - 42 [j_3(z+T) + j_3(z-T)] \right\},
 \end{aligned}$$

$$\tilde{\Xi}_7(z) = j_0(z+T) + j_0(z-T) + \frac{5}{2} [j_2(z+T) + j_2(z-T)] \tag{A7}$$

$$\begin{aligned}
 & -\frac{3}{4T} \left\{ 3 [j_1(z+T) - j_1(z-T)] - 7 [j_3(z+T) - j_3(z-T)] \right\} \\
 & -\frac{45h}{T^2} [j_2(z) - 6j_4(z)],
 \end{aligned}$$

$$\frac{1}{i} \tilde{\Xi}_8(z) = j_0(z+T) - j_0(z-T) + \frac{5}{2} [j_2(z+T) - j_2(z-T)] + \tag{A8}$$

$$\begin{aligned}
 & \frac{3}{4T} \left\{ 3 [j_1(z+T) + j_1(z-T)] - 7 [j_3(z+T) + j_3(z-T)] \right\} + \\
 & \frac{3h}{T} [3j_1(z) - 7j_3(z) + 11j_5(z)],
 \end{aligned}$$

$$\tilde{\Xi}_9(z) = \frac{3}{T} \left\{ j_1(z+T) - j_1(z-T) + \frac{7}{2} [j_3(z+T) - j_3(z-T)] \right\} \tag{A9}$$

$$\begin{aligned}
 & -\frac{15}{4T^2} \left\{ [j_0(z+T) + j_0(z-T)] - 5 [j_2(z+T) + j_2(z-T)] \right\} \\
 & -\frac{15h}{T^2} [j_0(z) - 5j_2(z) + 9j_4(z)],
 \end{aligned}$$

$$\frac{1}{i} \tilde{\Xi}_{10}(z) = -\frac{3}{T} \left\{ [j_1(z+T) + j_1(z-T)] + \frac{7}{2} [j_3(z+T) + j_3(z-T)] \right\} \tag{A10}$$

$$\begin{aligned}
 & -\frac{15}{4\mathbb{T}^2} \left\{ j_0(z + \mathbb{T}) - j_0(z - \mathbb{T}) - 5 [j_2(z + \mathbb{T}) - j_2(z - \mathbb{T})] \right\} + \\
 & \frac{15h}{\mathbb{T}^3} [-18j_1(z) + 77j_3(z) - 220j_5(z)] ,
 \end{aligned}$$

$$\begin{aligned}
 \tilde{\Xi}_{11}(z) &= -\frac{15}{2\mathbb{T}^2} [j_2(z + \mathbb{T}) + j_2(z - \mathbb{T})] \\
 &+ \frac{15}{4\mathbb{T}^3} \left\{ 3 [j_1(z + \mathbb{T}) - j_1(z - \mathbb{T})] - 7 [j_3(z + \mathbb{T}) - j_3(z - \mathbb{T})] \right\} + \\
 &\frac{15h}{\mathbb{T}^4} [2j_0(z) + 5j_2(z) - 72j_4(z)] ,
 \end{aligned} \tag{A11}$$

$$\begin{aligned}
 \frac{1}{i} \tilde{\Xi}_{12}(z) &= -\frac{15}{2\mathbb{T}^2} [j_2(z + \mathbb{T}) - j_2(z - \mathbb{T})] \\
 &- \frac{15}{4\mathbb{T}^3} \left\{ 3 [j_1(z + \mathbb{T}) + j_1(z - \mathbb{T})] - 7 [j_3(z + \mathbb{T}) + j_3(z - \mathbb{T})] \right\} + \\
 &- \frac{15h}{\mathbb{T}^3} [3j_1(z) - 7j_3(z) + 11j_5(z)] ,
 \end{aligned} \tag{A12}$$

$$\begin{aligned}
 \tilde{\Xi}_{13}(z) &= -\frac{35}{2\mathbb{T}^3} [j_3(z + \mathbb{T}) - j_3(z - \mathbb{T})] + \\
 &\frac{35}{4\mathbb{T}^4} \left\{ j_0(z + \mathbb{T}) + j_0(z - \mathbb{T}) - 5 [j_2(z + \mathbb{T}) + j_2(z - \mathbb{T})] \right\} + \\
 &\frac{35h}{\mathbb{T}^4} [j_0(z) - 5j_2(z) + 9j_4(z)] ,
 \end{aligned} \tag{A13}$$

$$\begin{aligned}
 \frac{1}{i} \tilde{\Xi}_{14}(z) &= \frac{35}{2\mathbb{T}^3} [j_3(z + \mathbb{T}) + j_3(z - \mathbb{T})] + \\
 &\frac{35}{4\mathbb{T}^4} \left\{ j_0(z + \mathbb{T}) - j_0(z - \mathbb{T}) - 5 [j_2(z + \mathbb{T}) - j_2(z - \mathbb{T})] \right\} + \\
 &\frac{105h}{\mathbb{T}^5} [4j_1(z) - 21j_3(z) + 66j_5(z)] .
 \end{aligned} \tag{A14}$$

APPENDIX B: ASYMPTOTIC BEHAVIOUR OF THE DUAL FUNCTIONS NEAR ZERO FREQUENCY

In this appendix we give the asymptotic behaviour of the dual functions near zero frequency. They are as follows:

$$\tilde{\Xi}_1(f) = \tilde{\xi}_1(z) , \quad \tilde{\xi}_1(z) = j_0(z) + \frac{5}{2}j_2(z) + \frac{27}{8}j_4(z) , \tag{B1}$$

$$\frac{1}{i}\tilde{\Xi}_2(f) = -\frac{3}{T}\tilde{\xi}_2(z), \quad \tilde{\xi}_2(z) = j_1(z) + \frac{7}{2}j_3(z) + \frac{55}{8}j_5(z), \quad (\text{B2})$$

$$\tilde{\Xi}_3(f) = -\frac{15}{2T^2}\tilde{\xi}_3(z), \quad \tilde{\xi}_3(z) = j_2(z) + \frac{9}{2}j_4(z), \quad (\text{B3})$$

$$\frac{1}{i}\tilde{\Xi}_4(f) = \frac{35}{2T^3}\tilde{\xi}_4(z), \quad \tilde{\xi}_4(z) = j_3(z) + \frac{11}{2}j_5(z), \quad (\text{B4})$$

$$\tilde{\Xi}_5(f) = \frac{315}{8T^4}\tilde{\xi}_5(z), \quad \tilde{\xi}_5(z) = j_4(z), \quad (\text{B5})$$

$$\frac{1}{i}\tilde{\Xi}_6(f) = -\frac{693}{8T^5}\tilde{\xi}_6(z), \quad \tilde{\xi}_6(z) = j_5(z), \quad (\text{B6})$$

$$\tilde{\Xi}_7(f) = -\frac{45h}{T^2}\tilde{\xi}_7(z), \quad \tilde{\xi}_7(z) = j_2(z) - 6j_4(z) - \frac{1}{15}z \sin z, \quad (\text{B7})$$

$$\frac{1}{i}\tilde{\Xi}_8(f) = \frac{9h}{T}\tilde{\xi}_8(z), \quad \tilde{\xi}_8(z) = j_1(z) - \frac{7}{3}j_3(z) + \frac{11}{3}j_5(z) - \frac{1}{3}\sin z, \quad (\text{B8})$$

$$\tilde{\Xi}_9(f) = -\frac{15h}{T^2}\tilde{\xi}_9(z), \quad \tilde{\xi}_9(z) = j_0(z) - 5j_2(z) + 9j_4(z) - \cos z, \quad (\text{B9})$$

$$\frac{1}{i}\tilde{\Xi}_{10}(f) = -\frac{270h}{T^3}\tilde{\xi}_{10}(z), \quad \tilde{\xi}_{10}(z) = j_1(z) - \frac{77}{18}j_3(z) + \frac{110}{9}j_5(z) - \frac{5}{18}\sin z - \frac{1}{18}z \cos z, \quad (\text{B10})$$

$$\tilde{\Xi}_{11}(f) = \frac{30h}{T^4}\tilde{\xi}_{11}(z), \quad \tilde{\xi}_{11}(z) = j_0(z) + \frac{5}{2}j_2(z) - 36j_4(z) - \frac{1}{2}z \sin z - \cos z, \quad (\text{B11})$$

$$\frac{1}{i}\tilde{\Xi}_{12}(f) = -\frac{45h}{T^3}\tilde{\xi}_{12}(z), \quad \tilde{\xi}_{12}(z) = j_1(z) - \frac{7}{3}j_3(z) + \frac{11}{3}j_5(z) - \frac{1}{3}\sin z, \quad (\text{B12})$$

$$\tilde{\Xi}_{13}(f) = \frac{35h}{T^4}\tilde{\xi}_{13}(z), \quad \tilde{\xi}_{13}(z) = \tilde{\xi}_9(z), \quad (\text{B13})$$

$$\frac{1}{i}\tilde{\Xi}_{14}(f) = \frac{420h}{T^5}\tilde{\xi}_{14}(z), \quad \tilde{\xi}_{14}(z) = j_1(z) - \frac{63}{12}j_3(z) + \frac{33}{2}j_5(z) - \frac{1}{4}\sin z - \frac{1}{12}z \cos z, \quad (\text{B14})$$

where $h = (-1)^N$.

APPENDIX C: ASYMPTOTIC BEHAVIOUR OF THE DUAL FUNCTIONS NEAR ORBITAL FREQUENCY

The leading terms in the asymptotic expansions of the dual functions $\tilde{\Xi}_a(z)$ near the orbital frequency are as follows:

$$\tilde{\Xi}_1(f) = -\frac{45h}{8T}\tilde{\xi}_1(y), \quad \tilde{\xi}_1(y) = j_1(y) - \frac{7}{3}j_3(y) - \frac{1}{3}\sin y, \quad (\text{C1})$$

$$\frac{1}{i}\tilde{\Xi}_2(f) = -\frac{105h}{8T^2}\tilde{\xi}_2(y), \quad \tilde{\xi}_2(y) = j_0(y) - 5j_2(y) - \cos y, \quad (\text{C2})$$

$$\tilde{\Xi}_3(f) = -\frac{14}{T^3}\tilde{\xi}_3(y), \quad \tilde{\xi}_3(y) = \tilde{\xi}_1(y) \quad (\text{C3})$$

$$\frac{1}{i}\tilde{\Xi}_4(f) = -\frac{6}{T^4}\tilde{\xi}_4(y), \quad \tilde{\xi}_4(y) = \tilde{\xi}_2(y), \quad (\text{C4})$$

$$\tilde{\Xi}_5(f) = \frac{21}{T^5}\tilde{\xi}_5(y), \quad \tilde{\xi}_5(y) = \tilde{\xi}_1(y), \quad (\text{C5})$$

$$\frac{1}{i}\tilde{\Xi}_6(f) = \frac{33}{5T^6}\tilde{\xi}_6(y), \quad \tilde{\xi}_6(y) = \tilde{\xi}_2(y), \quad (\text{C6})$$

$$\tilde{\Xi}_7(f) = \tilde{\xi}_7(y), \quad \tilde{\xi}_7(y) = j_0(y) + \frac{5}{2}j_2(y), \quad (\text{C7})$$

$$\frac{1}{i}\tilde{\Xi}_8(f) = \tilde{\xi}_8(y), \quad \tilde{\xi}_8(y) = -\tilde{\xi}_7(y), \quad (\text{C8})$$

$$\tilde{\Xi}_9(f) = -\frac{3}{T}\tilde{\xi}_9(y), \quad \tilde{\xi}_9(y) = j_1(y) + \frac{7}{2}j_3(y), \quad (\text{C9})$$

$$\frac{1}{i}\tilde{\Xi}_{10}(f) = \frac{1}{T}\tilde{\xi}_{10}(y), \quad \tilde{\xi}_{10}(y) = \tilde{\xi}_9(y), \quad (\text{C10})$$

$$\tilde{\Xi}_{11}(f) = -\frac{15}{2T^2}\tilde{\xi}_{11}(y), \quad \tilde{\xi}_{11}(y) = j_2(y), \quad (\text{C11})$$

$$\frac{1}{i}\tilde{\Xi}_{12}(f) = \frac{1}{T^2}\tilde{\xi}_{12}(y), \quad \tilde{\xi}_{12}(y) = -\tilde{\xi}_{11}(y), \quad (\text{C12})$$

$$\tilde{\Xi}_{13}(f) = \frac{35}{2T^3}\tilde{\xi}_{13}(y), \quad \tilde{\xi}_{13}(y) = j_3(y), \quad (\text{C13})$$

$$\frac{1}{i}\tilde{\Xi}_{14}(f) = \frac{1}{T^3}\tilde{\xi}_{14}(y), \quad \tilde{\xi}_{14}(y) = \tilde{\xi}_{13}(y). \quad (\text{C14})$$

where $y = z - T$.

APPENDIX D: PLOTS OF THE FOURIER TRANSFORM OF AUTOCOVARANCE FUNCTION

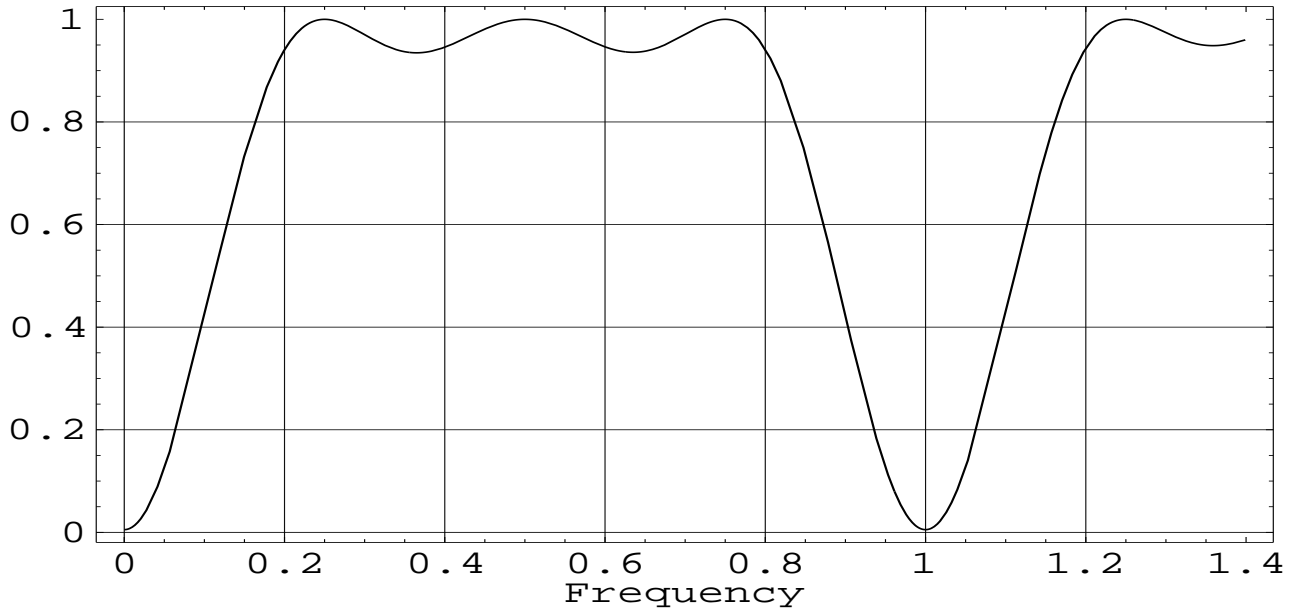


Figure D1. Plot of the Fourier transform of the filter function of timing residuals for the amount of orbital revolutions $N = 4$. Frequency is measured in units of orbital frequency n_b . Amplitude of the transform has been normalized to unity.

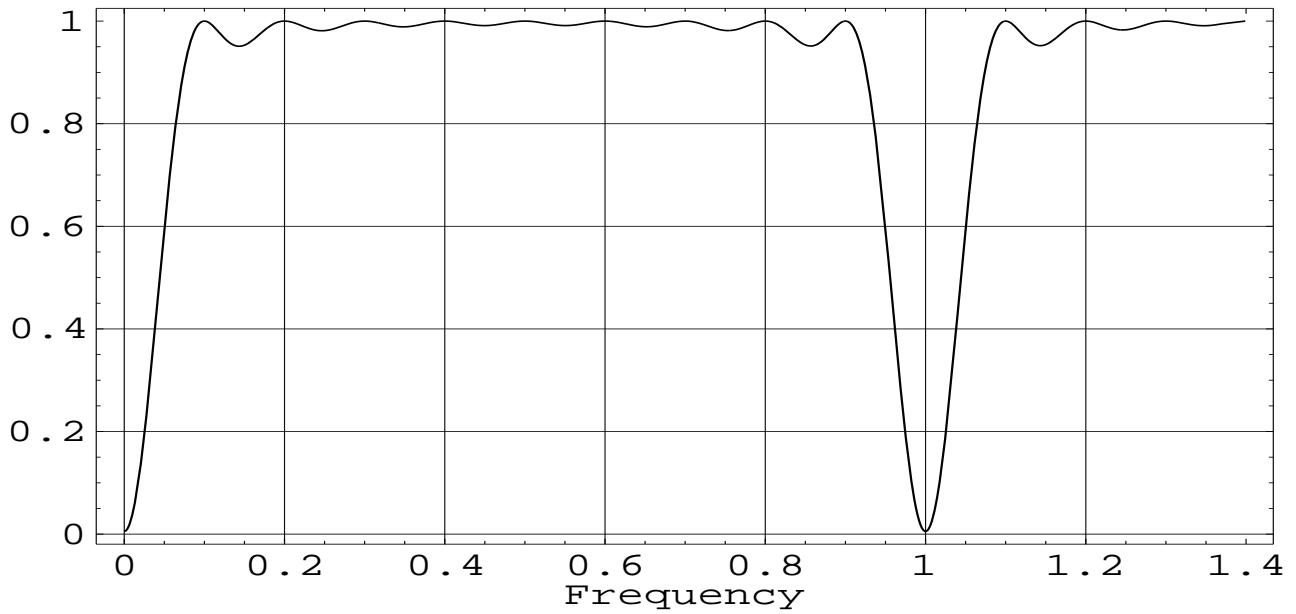


Figure D2. Plot of the Fourier transform of the filter function of timing residuals for the amount of orbital revolutions $N = 10$. Frequency is measured in units of orbital frequency n_b . Amplitude of the transform has been normalized to unity.

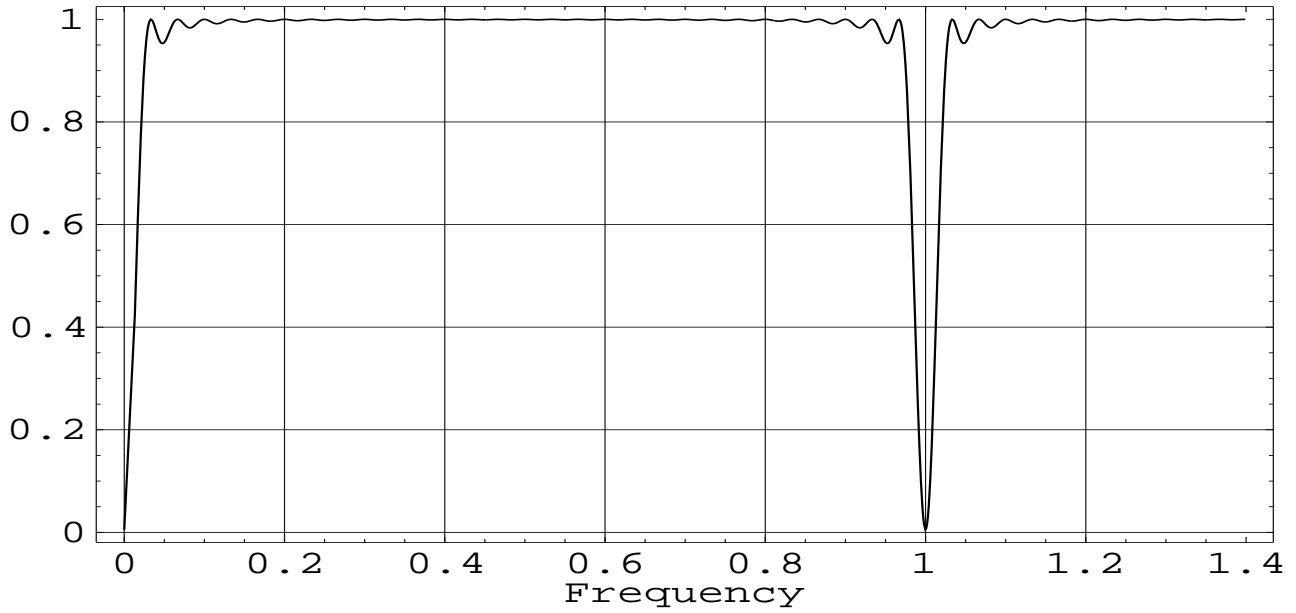


Figure D3. Plot of the Fourier transform of the filter function of timing residuals for the amount of orbital revolutions $N = 30$. Frequency is measured in units of orbital frequency n_b . Amplitude of the transform has been normalized to unity.